Field Enhancement and Work Function Difference of IrO_2 Nano-Emitter Arrays using EFM and SKPM Spectroscopy

D. C.-S. Chiang*, Z.-F.P. Lei* , R. Barrowcliff**, F. Zhang**

* Washington State University Vancouver, WA 98686, USA, dcschiang@yahoo.com.tw
** Sharp Labs of America, Camas, WA, USA, FZhang@sharplabs.com

ABSTRACT

We have observed spatial variation of two important physical properties related to field emission (work function and field enhancement factor) of IrO_2 nanorod emitter arrays using spectroscopy methods of electric force microscope (EFM) and scanning Kelvin probe microscope (SKPM). IrO_2 nanorod arrays have been considered an outstanding material for next-generation flat panel display due to their relatively high conductivity, inertness to oxygen, and low threshold field. The spacing, radius, and morphology of the nanoprotrusions were observed to change significantly within the sample. The Largest force gradients (or field enhancement) were observed in areas with nanorods of smallest radius and densest population. Difference of work function is also observed between high and low density region. The discrepancy of larger than 0.5 eV of the work function may result in difference of emission current by three orders of magnitude between high density and low-density areas of the nanorod arrays.

Keywords: field emission, field enhancement, work function, electric force microscope, scanning Kelvin probe microscope

1 INTRODUCTION

The material properties of IrO_2 render them quite attractive for field emitting applications. From literature, it is found that IrO_2 has a comparable electrical conductivity with its metallic component iridium, which is around 32 μΩ-cm [1]. Unlike metallic or refractory emitters, IrO_2 is already a stable oxide yielding them chemically inert and less susceptible to reactions with oxygen [2]. IrO_2 has also shown to have a low threshold field (E_{th} ~5.6 V/μm) and a large field enhancement (β~40000), which are comparable to N-doped diamond films and carbon nanotube films [3]. It has been shown from Fowler-Nordheim that the work function and the electric field are the tow main factors that determine the field emission current of materials. The work function is dependent on the material itself and the latter is a function of the morphology and spatial distribution. In this paper, the variation of the electrostatic forces produced by the IrO_2 nanorods under an applied sample bias are investigated using the electrostatic force microscope (EFM) spectroscopy, and the work function variation is studied using scanning Kelvin probe spectroscopy.

2 EFM AND SKPM

We use EFM [4,5]to measure the changes of the vibration amplitude of the AFM cantilever due to the existence of the electric force gradient. The electric force gradient is generated because the electric field exists when a voltage difference between the EFM probe and the sample is applied. From the theory of cantilever vibration [6,7,8], the change in amplitude is proportional to the force gradient as shown in equation (1).

$$\frac{dF}{dZ} = \frac{3\sqrt{3}(\Delta A)k}{-2QA_o} \qquad (1)$$

Fig. 1 shows the spectroscopy curve of the vibration amplitude as a function of the height of the probe. It is clearly seen that the vibration amplitude decreases significantly due to the voltage difference between the probe and the sample.

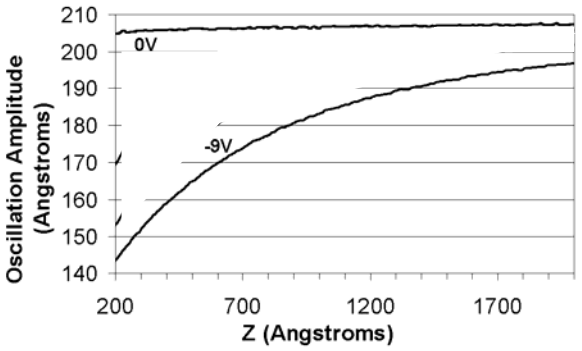

Fig. 1 The vibration amplitude of a cantilever as a function of the probe height. A significant reduction of the amplitude is observed when a bias voltage of -9 volts is applied to the probe with respect to the sample.

In SKPM [9,10,11,12] measurements, the potential difference between the probe and the sample
Is a V_{dc} overlapped with a V_{ac}

$$V_{tip} = V_{dc} + V_{ac} Sin(\omega t) \quad (2)$$

From the theory of electrostatics, the first harmonic of the capacitive force that results from this applied bias voltage V_{tip} is given by

$$F_{Cap\omega} = \left(\frac{dC}{dZ}\right)\left(V_{dc} - \Phi(x)\right) V_{ac} Sin(\omega t) \quad (3)$$

Where *C* is the tip to surface capacitance and Φ(x) is the contact potential difference (or work function difference) between the tip and the surface. Based upon equation (3), if V_{dc} equal to the contact potential difference Φ(x), then $F_{Cap\omega}$ is equal to zero, i.e. the first harmonic of the vibration amplitude of the cantilever is also zero. So by finding V_{dc} that results in zero of the vibration amplitude, the work function difference, and thus the work function variation through the surface of different morphology can be determined. An example of SKPM curve of the cantilever's vibration amplitude as a function of V_{dc} for HOPG is shown in Fig. 2. The contact potential difference in this case is ~18mV.

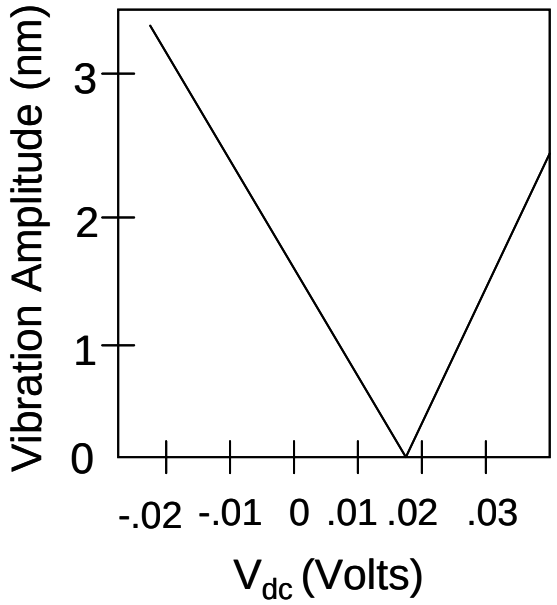

Fig. 2, Vibration amplitude of the cantilever as a function of V_{dc}. It is clearly shown that the contact potential differenc is 18mV, where the vibration amplitude vanishes.

3. IrO_2 NANOROD ARRAYS

The IrO_2 nanorod arrays were grown on a silicon (100) substrate. The procedure consists of coating the silicon substrate with a titanium film to serve as a growth promotion layer for the IrO_2 nanorods; then catalyst particles comprising of (Methylcyclopentadienyl) (1, 5-cyclooctadiene) iridium are evenly dispersed on the titanium coated silicon substrate and inserted into a chemical vapor deposition chamber (CVD) to undergo the growing process. The CVD chamber is purged with oxygen until it reaches a pressure of 30-50 Torr with a deposition temperature of 300°-400°C. This CVD process produces nanorods aligned in close proximity with each other, thus forming arrays[8]. IrO_2 nanorod arrays with three distinct regions that have varying nanorod density, size, and morphology are clearly shown in SEM and AFM images. The first region is termed dense region because of the large quantity of nanorods populating it with a fairly uniform size. The second region is called least dense region. The nanorods in this region are more sparsely distributed. It is interesting that the sample also has a region where the nanorods are very thin and densely packed. In this region the nanorods are so tightly packed that they tend to cluster together forming petal-like clusters of IrO_2 nanorods. Therefore the name cluster zone was coined to this region of the sample.

3 RESULTS AND DISCUSSION

Three different regions of the IrO_2 nanorod array were investigated with the scanning probe microscope by means of EFM and SKPM spectroscopy to measure the electric force gradient and contact potential difference. These regions are the least dense, dense, and flower cluster regions of the IrO_2 nanorod array. The semi contact AFM topographical images of the nanorod array were obtained first before conducting EFM and SKPM experiments.

Region	Flower cluster		Least dense		Densest
Location	A	B	A	B	
Force gradient (10-3 N/m)	9.0	8.9	12.1	6.2	1.1
Field enhancement γ	Large		Large		small

Table I. Dynamic EFM measurements on the force gradient exerted on the cantilever by the different IrO_2 nanorod arrays.

Table 1 shows the magnitude of the electrostatic force gradient exerted on the cantilever by the different regions of the IrO_2 nanorod array. The tip-sample separation distance *Z* was 30nm with an applied sample bias -9V. It is evident from table 1 that the IrO_2 nanorods found in the cluster zone have the largest magnitude of the force gradient as measured by the cantilever. Also, it is observed from table 1 that the electrostatic forces gradient exerted on the cantilever by the biased nanorods on the different regions

follow the subsequent descending order from largest to smallest *F*: cluster, least-dense, and dense. This descending sequence was also observed when a sample bias of -6V was applied. Based upon this experimental result, it is appropriate to conclude that the field enhancement factor γ is large, medium, and small for the cluster region, low density region, and high density region respectively. The field enhancement factor γ shown in the bottom of Table I is defined as

$$\gamma = \frac{E}{V} \qquad (2)$$

where *E* is the electric field (proportional to the measured electrostatic force), and V is the bias voltage between the sample and the probe tip.

The fairly consistent observation that the field enhancement is strongly dependent upon the morphology of the nanorod arrays was reported by Jo *et al* [13] and Nilsson *et al* [14]. As can be seen from table I, the nanorods in the least-dense region produced a larger electrostatic force as compared to the nanorods in the dense region. Notice that the spacing between nanorods in the least-dense region is larger than those in the dense region, and the radius of nanorods in the least-dense is smaller than those in the dense region. In contrast, the nanorods in the cluster region possess extremely small radiuses. The effect on the field enhancement factor by the spacing and radius of nanorods can be best understood by looking at the field penetration or screening effect reported by Nilsson's group [14]. Using the field penetration model, the least-dense zones show greater field than the dense area as measured because of the increase in the field enhancement factor due to the larger spacing between the nanorods [14]. The nanorods in the cluster region exerted the largest amount of force. This larger magnitude of *F* in this region can be attributed to the extremely small radiuses and sharper nanorod tips compared to the apexes of the nanorods found in the dense or least dense regions.

The contact potential difference is also estimated using SKPM spectroscopy curves in each region of the nanorod array. Quantitatively, there exists a larger than 0.5 eV discrepancy of work function between high and low density areas. This discrepancy can be attributed to two main factors: the different characteristics of the adsorption layer present in each region, and differences in materials properties such as the crystal structure or chemical composition. The variations of the work function is usually greatly manifested when it is caused by the material itself such as differences in the crystal structure or chemical composition, in particular, the distribution of the surface crystal facets.

It is important to note that a small change in the work function of the nanorods can produce a large change in the field emission current. The contact potential difference of the low density area is about 0.5 eV lower than that of high density area (including both dense and flower cluster area). This result implies that the work function of the high density area is 0.5 eV higher than that of low density area. The magnitude of *J* was calculated with the different values for the IrO_2 nanorod work function and an applied electric field of $E = 15V/\mu m$. From our measurements, the work function of IrO_2 nanorod emitters in the high density or flower cluster area is 0.5 eV larger than that of the low density area. The emission current in the high density area will be lower that that of the low density area by three orders of magnitude based upon the smaller value of the work function.

4 CONCLUSION

The value of the work function in the higher density areas of the IrO_2 nanorod emitter arrays was found to be 0.5 eV larger than that of low density areas based upon the contact potential difference measured by the SKPM spectroscopy method. This can most likely be related to the effect that different crystal structures, crystal facets, and chemical purity may exist in the different density regions of the nanorod emitter arrays Since the field emission current is a strong function of the work function of the IrO_2 nanorods, It is observed that a decrease of 0.5eV in the work function of the low nanorod density areas may result in the increase of the field emission current by three orders of magnitude as compared with the emission current of the high density areas. The magnitudes of the electrostatic force gradients change in these three typical areas of the IrO_2 nanorod array. The EFM spectroscopy data indicated that the regions with the least-dense population of nanorods yielded the largest force gradients whereas the densest regions yielded a lower force gradient. This phenomena can be explained using the model of field penetration.

REFERENCES

[1] W.D. Ryden, A.W. Lawson, and C.C. Sartain, Phys. Rev. B **1**, 1494 (1970)

[2] B.R. Chalamala, R.M. Wallace, and B.E. Gnade, J. Vac. Sce. Technol. B **16**, 2859 (1998)

[3] R.-S. Chen and Y-S Huang, et al. "Field emission from vertically aligned conductive IrO2 nanorods" Appl. Phys. Lett. **84**, 1552 (2004)

[4] R.A. Said "Perturbation detection of electric force gradients using the phase shift method." J. Phys. D: Appl. Phys. **34** L7 (2001).

[5] J. Chu, T. Itoh, C. Lee, and T. Suga. "Novel high vacuum scanning force microscope using a piezoelectric cantilever and the phase detection method." J. Vac. Sci. Techonl. B 15, 1551 1997.

[6] T.R. Albrecht, P. Grutter, D. Horne, and D. Rugar. "Frequency modulation detectionusing high-Q cantilevers for enhance force microscope sensitivity." J. Appl. Phys. **69** ,668 1991.

[7] Y. Martin, C.C. Williams, and H.K. Wickramasinghe. "Atomic force microscope-force mapping and profiing on a sub 100-Angstrom scale." J. Appl. Phys. **61**, 4723 1987.
[8] Y. Martin, et al. "High-resolution capacitance measurement and potentiometry by force microscopy." Appl. Phys. Lett. **52**, 1103 1988.
[9] M. Nonnenmacher, M.P. O'Boyle, and H. K. Wickramasinghe, Appl. Phys. Lett. **58**, 2921 (1991).
[10] H. O. Jacobs, H.F. Knnap, S. Muller, and A. Stemmer, Ultramicroscopy, **69**, 39-49 (1997).
[11] G. Koley and M.G. Spencer, J. Appl. Phys. **90,** 337-344 (2001).
[12] M. P. O'Boyle, T. T. Huang, and H. K. Wickramasinghe, Appl. Phys. Lett. **74**, 2641 (1999).
[13] S. H. Jo, Y. Tu, Z. P. Huang, D. L. Carnahan, D. Z. Wang, and Z. F. Ren. Appl. Phys. Lett. **82**, 3520 (2003).
[14] L. Nilsson, O. Groening, C. Emmenegger, O. Kuettel, E. Schaller, L. Schlapbach, H. Kind, J. M. Bonard, K. Kern. Appl. Phys. Lett. **76**, 2071 (2000).